Research Square

Preprints are preliminary reports that have not undergone peer review.
They should not be considered conclusive, used to inform clinical practice,
or referenced by the media as validated information.

Forensic BTEX Speciation, Directional Conditional Probability Function (CPF) Plume Characterization, and Concentration-Based Inhalation Carcinogenic Risk Assessment Across 13 Urban Microclimates

Saptarshi Sadhu

saptarshi1.sadhu@stu.adamasuniversity.ac.in

Adamas University https://orcid.org/0009-0009-7505-1973

Research Article

Keywords: Benzene carcinogenicity, BTEX speciation, Conditional Probability Function, Ozone Formation Potential, Incremental Lifetime Cancer Risk, Lower Gangetic Plain

Posted Date: November 20th, 2026

DOI: https://doi.org/10.21203/rs.3.rs-11793630/v1

License: This work is licensed under a Creative Commons Attribution 4.0 International License.
Read Full License

Additional Declarations: The authors declare no competing interests.

Forensic BTEX Speciation, Directional Conditional Probability Function (CPF) Plume Characterization, and Concentration-Based Inhalation Carcinogenic Risk Assessment Across 13 Urban Microclimates

Saptarshi Sadhu[1*]

[1]School of Engineering and Technology, Adamas University, Kolkata 700126, India

ORCID: https://orcid.org/0009-0009-7505-1973

*Correspondence: saptarshi1.sadhu@stu.adamasuniversity.ac.in

Abstract

Speciated monoaromatic hydrocarbons—benzene, toluene, ethylbenzene, and xylenes (BTEX)—govern urban photochemical oxidation while imposing severe carcinogenic inhalation risks. We investigate BTEX speciation, photochemical reactivity, diagnostic emission ratios, Conditional Probability Function (CPF) directional polar vectors, and inhalation health risks across 13 continuous monitoring stations in Kolkata and Howrah during 2024–2025 (721,193 valid observations). Monoaromatic loading ($\sum$BTEX) spanned from 8.02 μg m^{-3} at parkland background (Fort William) to 40.03 μg m^{-3} at industrial foundries (Dasnagar). Deconstruction of observational periodicity established that Dasnagar's apparent inter-annual decline was an artifact of winter-only monitoring in 2024; matched-period comparisons confirmed a moderate 14.7% change (40.03 to 34.17 μg m^{-3}). Ambient benzene exceeded statutory benchmarks (5.0 μg m^{-3}) at four full-year stations and two seasonal records in 2024, peaking at Jadavpur (18.07 μg m^{-3}). Under the Inhalation Unit Risk framework of the World Health Organization (WHO) and United States Environmental Protection Agency Risk Assessment Guidance for Superfund (USEPA RAGS Part F), Incremental Lifetime Cancer Risk ranged from 8.94×10^{-6} to 108.43×10^{-6} (1.08×10^{-4} at Jadavpur), universally exceeding the 1×10^{-6} de minimis threshold network-wide and surpassing the 1×10^{-4} intolerable risk benchmark at congested intersections. While benzene drives 100% of the quantified unit-risk carcinogenic burden, toluene and xylenes generate $>85\%$ of BTEX-derived Ozone Formation Potential (up to 184.06 μg m^{-3}). Directional CPF analysis showed high-

CPF westerly sectors consistent with possible industrial foundry and solvent influence across the Hooghly River alongside north-northeasterly regional drainage.

Keywords: Benzene carcinogenicity; BTEX speciation; Conditional Probability Function; Ozone Formation Potential; Incremental Lifetime Cancer Risk; Lower Gangetic Plain.

1 Introduction

1.1 Atmospheric Significance and Oxidation Chemistry of Urban VOCs

Volatile organic compounds (VOCs) represent fundamental chemical constituents of the troposphere that dictate urban air quality, photochemical smog dynamics, and regional climate forcing (Monks et al., 2015; Sillman and He, 2002). In polluted boundary layers, non-methane hydrocarbons undergo rapid photooxidation initiated primarily by the hydroxyl radical (OH) during daytime, nitrate radicals (NO_3) at night, and ozone (O_3) across diurnal cycles (Atkinson and Arey, 2003). Among the complex suite of hundreds of organic compounds present in urban atmospheres, monoaromatic hydrocarbons—specifically Benzene, Toluene, Ethylbenzene, *m*, *p*-Xylene, and *o*-Xylene, collectively designated as BTEX—constitute a major fraction (20%–60%) of total non-methane volatile organic carbon in South Asian and East Asian megacity airsheds (Barletta et al., 2005; Ho et al., 2004; Mondal et al., 2023).

The oxidation mechanisms of alkylbenzenes proceed via competitive pathways of OH-radical addition to the aromatic ring and hydrogen-atom abstraction from alkyl substituents (Calvert et al., 2002; Atkinson and Arey, 2003). Ring addition generates hydroxycyclohexadienyl-type peroxy radicals that react with molecular oxygen and nitrogen oxides ($NO_x \equiv NO + NO_2$), converting nitric oxide (NO) to nitrogen dioxide (NO_2) without ozone consumption. Subsequent photolysis of NO_2 yields ground-state oxygen atoms ($O(^3P)$), driving the net catalytic production of tropospheric ozone:

$$RH + OH + O_2 \longrightarrow RO_2 + H_2O \tag{1}$$

$$RO_2 + NO \longrightarrow RO + NO_2 \tag{2}$$

$$NO_2 + h\nu \longrightarrow NO + O(^3P) \quad (\lambda < 424\ \text{nm}) \tag{3}$$

$$O(^3P) + O_2 + M \longrightarrow O_3 + M \tag{4}$$

Simultaneously, oxygenated ring-cleavage intermediates (such as glyoxal, methylglyoxal, and unsaturated dicarbonyls) and phenolic ring-retaining species (phenol, cresols, nitrophenols) exhibit low saturation vapor pressures, condensing onto pre-existing seed aerosols to generate secondary organic aerosols (SOA) (Volkamer et al., 2010; Camredon et al., 2007). In subtropical megacities characterized by high solar actinic flux and substantial

background NO_x loadings, monoaromatic hydrocarbons thereby serve as primary chemical catalysts for secondary oxidant formation and haze aggravation (Tan et al., 2019; Xue et al., 2014).

1.2 Toxicological Foundations and Molecular Mechanisms of BTEX Species

Beyond their atmospheric reactivity, BTEX monoaromatics represent ubiquitous environmental toxicants with distinct toxicological, hematological, and carcinogenic mechanisms (WHO, 2010; Deguen and Zmirou-Navier, 2010). Benzene (C_6H_6, CAS No. 71-43-2) is classified by the International Agency for Research on Cancer (IARC, 2018) and the United States Environmental Protection Agency (USEPA, 1989) as a known Group 1 / Group A human carcinogen. Unlike threshold chemical toxicants, benzene exhibits non-threshold clastogenic and genotoxic leukemogenic properties (Smith, 2010). Inhalation represents the predominant pathway of human environmental exposure. Absorbed benzene undergoes hepatic bioactivation catalyzed primarily by cytochrome P450 2E1 (CYP2E1), yielding benzene oxide, which exists in equilibrium with oxepin (Lan et al., 2004). Subsequent spontaneous non-enzymatic rearrangement produces phenol, which is further hydroxylated by CYP2E1 to hydroquinone and catechol. Myeloperoxidase (MPO) in bone marrow progenitor cells oxidizes these phenolic intermediates to 1,4-benzoquinone and 1,2-benzoquinone, which directly inhibit topoisomerase II, disrupt mitotic spindle microtubule assembly, and induce severe oxidative DNA damage, sister chromatid exchanges, and chromosomal aneuploidies (Smith, 2010; IARC, 2018). Specific chromosomal abnormalities consistently documented in benzene-exposed cohorts include loss of chromosomes 5 and 7 ($-5/-7$, del(5q)/del(7q)) and reciprocal translocations $t(8;21)$ and $t(15;17)$, characteristic of acute myeloid leukemia (AML), myelodysplastic syndromes (MDS), and aplastic anemia (Lan et al., 2004; WHO, 2010).

Conversely, toluene (C_7H_8), ethylbenzene (C_8H_{10}), and xylene isomers (C_8H_{10}) exhibit lower carcinogenic potency but induce marked central nervous system (CNS) depression, neurobehavioral impairments, ototoxicity, and respiratory mucosal irritation (Kumar et al., 2018). Toluene is rapidly oxidized by side-chain hydroxylation to benzyl alcohol, followed by oxidation to benzoic acid and conjugation with glycine to form hippuric acid, which is cleared renally without forming genotoxic quinone complexes. Ethylbenzene is classified by IARC as a Group 2B possible human carcinogen based on rodent alveolar and renal adenomas, whereas xylenes are classified in Group 3 (not classifiable as to human carcinogenicity). Nevertheless, chronic multi-compound BTEX exposure induces synergistic toxic effects, including enhanced cellular oxidative stress and competitive metabolic inhibition of CYP2E1 pathways, prolonging the internal residence time of benzene in circulating systemic circulation (Deguen and Zmirou-Navier, 2010; Batterman et al., 2020).

1.3 South Asian Airshed Dynamics and Urban Emission Typologies

The lower Gangetic plain of eastern India contains some of the most densely populated, commercially congested, and environmentally burdened urban agglomerations globally (Venkataraman et al., 2018; Balakrishnan et al., 2019). The twin metropolitan centers of Kolkata and Howrah (conurbation population > 16 million) occupy a flat deltaic landscape along the lower reaches of the tidally influenced Hooghly River, approximately 120 km north of the Bay of Bengal (Kar et al., 2020; Sarkar et al., 2020). The urban airshed exhibits a pronounced morphological dichotomy across the river corridor. The western bank (Howrah, Dasnagar, Ghusuri) has historically served as eastern India's primary foundry, metal casting, rolling mill, glass fabrication, and heavy chemical synthesis cluster (Karmakar, 2020). In contrast, the eastern bank (Kolkata) contains high-density commercial corridors, major academic and administrative institutions, transit hubs, and residential neighbourhoods characterized by extreme vehicular density (Chattopadhyay et al., 2010; Das et al., 2020).

Ambient BTEX emissions across this conurbation arise from multiple overlapping anthropogenic sources:

1. Vehicular Exhaust and Evaporative Losses: Fleet composition features a heavy proportion of two-stroke and four-stroke motorcycles, light commercial three-wheelers, diesel freight buses, and passenger cars operating in persistent stop-and-go congestion. Fuel distribution infrastructure historically suffered from evaporative fugitive losses due to inadequate vapor recovery systems (VRS) at retail dispensing outlets (Majumdar et al., 2011).

2. Industrial Solvent Evaporation and Metal Fabrication: Foundry cores, casting molds, industrial degreasing agents, surface coating lines, paint manufacturing units, and printing presses across Howrah release high volumes of toluene, xylenes, and aliphatic solvents directly into the boundary layer without catalytic thermal recovery (Srivastava et al., 2005; Rai et al., 2020).

3. Fuel Adulteration and Solid Fuel Combustion: Small-scale informal commercial units, kerbside food preparation vendors, and municipal solid waste open burning contribute unburned hydrocarbons and pyrogenic monoaromatics (Venkataraman et al., 2018; Dutta and Pal, 2022).

Compounding these emissions, the region experiences strong seasonal meteorological modulation (Kumar et al., 2018). During the post-monsoon and winter seasons (November to February), continental synoptic anticyclones establish persistent thermal inversions with nocturnal planetary boundary layer (PBL) heights descending below 150–200 m, accompanied by calm or sluggish wind speeds (< 1.5 m s^{-1}). These meteorological condi-

tions prevent vertical convective dispersion and trap toxic aromatic compounds within the shallow surface breathing zone (Ghosh et al., 2023; Roy et al., 2024).

1.4 Receptor-Oriented Directional Tracing: Conditional Probability Function

Identifying emission source regions in complex urban atmospheres requires decoupling meteorological advection from chemical emission intensity (Zhang et al., 2014). Traditional passive dispersion modeling and chemical transport simulations require highly detailed bottom-up gridded emission inventories, which are frequently unavailable or subject to large structural uncertainties in rapidly developing South Asian urban regions (Venkataraman et al., 2018).

Receptor-oriented directional techniques provide robust empirical alternatives. The Conditional Probability Function (CPF) is an established non-parametric diagnostic tool that couples high-frequency continuous pollutant concentration observations with synchronized horizontal wind direction vectors (Ashbaugh et al., 1985; Pekey and Yilmaz, 2011). By evaluating the conditional probability that a measured pollutant concentration from a specific wind direction sector exceeds a high-percentile threshold (typically the 75th, 85th, or 90th percentile), CPF polar plots effectively isolate the directional orientation of major emission plumes relative to the monitoring station head. Unlike unconstrained mean concentration roses, which can be distorted by isolated high-concentration calm-wind outliers, CPF polar vectors highlight consistent high-concentration transport corridors, providing directional fingerprints for regulatory source apportionment (Zhang et al., 2014; Xue et al., 2014).

1.5 Diagnostic Ratios and Photochemical Reactivity Metrics

Diagnostic concentration ratios between distinct hydrocarbon species furnish chemical fingerprints that identify dominant emission source categories and atmospheric photochemical processing (Ho et al., 2004; Barletta et al., 2005):

1. Toluene-to-Benzene (T/B) Ratio: The mass ratio of toluene to benzene is a widely recognized tracer for distinguishing vehicular combustion from industrial solvent evaporation (Tiwari et al., 2010; Mondal et al., 2023). T/B ratios between 0.4 and 1.2 characterize primary vehicular exhaust emissions from internal combustion engines. In contrast, T/B ratios exceeding 1.5 to 4.5 indicate prominent fugitive emissions from industrial solvent evaporation, painting, textile printing, and chemical synthesis, reflecting the high toluene content in commercial solvent formulations (Srivastava et al., 2005; Pekey and Yilmaz, 2011).

2. Xylene-to-Ethylbenzene (X/E) Ratio: Serves as a quantitative indicator of atmospheric photochemical aging (Monks et al., 2015). Because m,p-xylene reacts with hydroxyl radicals approximately three times faster than ethylbenzene ($k_{OH} \approx 23.6 \times 10^{-12}\,cm^3\,molecule^{-1}\,s^{-1}$ vs $7.0 \times 10^{-12}\,cm^3\,molecule^{-1}\,s^{-1}$ at 298 K), lower X/E ratios denote aged, advected air parcels, whereas higher ratios indicate fresh, local emissions (Atkinson and Arey, 2003).

3. Ozone Formation Potential (OFP): Ambient concentration alone does not represent the secondary photochemical ozone formation capability of individual VOC species. Using Carter's Maximum Incremental Reactivity (MIR) scale (Carter, 1994, 2010), individual species mass concentrations are weighted by their ozone generation capacity under ozone-sensitive conditions, decoupling toxicological mass loadings from photochemical oxidant generation.

1.6 Research Objectives and Scope of Investigation

Despite the recognized environmental and public health hazards of VOCs, previous atmospheric research in eastern India has focused predominantly on criteria particulate matter ($PM_{2.5}$, PM_{10}) and sulfur or nitrogen oxides (Kar et al., 2020; Sarkar et al., 2020; Das et al., 2020), with BTEX studies restricted to short-term passive sampling campaigns or single-station observations (Chattopadhyay et al., 2010; Majumdar et al., 2011). Comprehensive network-wide, multi-year, continuous chromatography datasets documenting speciated BTEX dynamics across diverse urban microclimates have remained unavailable.

In this investigation, we utilize continuous 15-minute telemetry records from all 13 CAAQMS stations in the Kolkata and Howrah conurbation across calendar years 2024 and 2025 (721,193 valid observations) to provide a rigorous, evidence-based assessment. Our specific research objectives are:

1. Quantify empirical speciation profiles of Benzene, Toluene, Ethylbenzene, m,p-Xylene, o-Xylene, and total monoaromatic loading ($\sum$BTEX) across 13 diverse microclimates, establishing strict stoichiometric closure.

2. Deconstruct observational periodicity and seasonal completeness to explain apparent inter-annual concentration variations and assess the impact of shallow winter boundary-layer inversion windows.

3. Characterize emission typologies using diagnostic T/B and X/E concentration ratios alongside photochemical reactivity and Ozone Formation Potential (OFP) modeling.

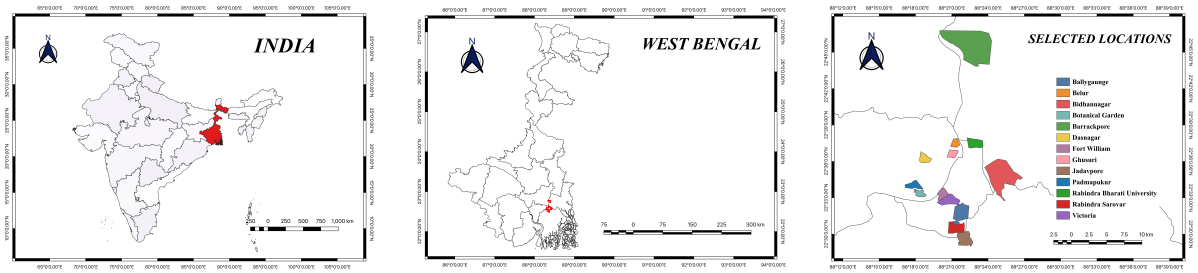
4. Map directional emission corridors via Conditional Probability Function (CPF) polar wind vectors, identifying trans-Hooghly transport and regional drainage flows.

5. Conduct quantitative inhalation carcinogenic and non-carcinogenic health risk assessments using contemporary concentration-based Inhalation Unit Risk frameworks (WHO and USEPA RAGS Part F), evaluating compliance with statutory Central Pollution Control Board (CPCB) standards.

2 Materials and Methods

2.1 Monitoring Network and Airshed Classification

The study domain encompasses the contiguous urban and peri-urban expanse of Kolkata and Howrah (22.45°N–22.80°N, 88.25°E–88.45°E), situated in the lower Gangetic delta at an average elevation of 3–9 m above mean sea level. The Hooghly River, a major distributary of the Ganges, bisects the metropolitan area longitudinally from north to south, creating a natural geographic boundary between the western industrial districts and the eastern commercial and residential grid.



(a) West Bengal in India (b) Study Area in West Bengal (c) 13 CAAQMS Monitoring Sites

Fig. 1 Geographic location of the study region and spatial layout of all 13 CAAQMS monitoring stations across the Kolkata and Howrah conurbation

Continuous atmospheric observations were obtained from the complete network of 13 Continuous Ambient Air Quality Monitoring System (CAAQMS) stations operated collaboratively by the West Bengal Pollution Control Board (WBPCB) and the Central Pollution Control Board (CPCB). Stations were sited in strict accordance with CPCB siting criteria (CPCB Guidelines for Ambient Air Quality Monitoring, 2003) and USEPA 40 CFR Part 58 regulatory requirements, with sample inlet heads situated between 3.5 m and 10.0 m above local ground level to capture human breathing-zone exposure without direct obstruction from adjacent building walls. Table 1 documents the validated geographic coordinates, elevation, land-use zoning classifications, primary emission drivers, and riverbank proximity for each station. The network captures six distinct urban microclimatic regimes: heavy industrial foundry clusters (Dasnagar, Ghusuri), dense vehicular/mixed urban intersections (Jadavpur, Ballygunge, Rabindra Bharati University), riverbank mixed industrial zones (Belur Math, Padmapukur), planned commercial/institutional zones (Bidhannagar), peri-urban industrial belts (Barrackpore SVSPA), and green parkland urban

background sites (Fort William, Victoria Memorial, Botanical Garden).

Table 1. Verified Metadata for all 13 CAAQMS Monitoring Stations in Kolkata and Howrah: Geodetic Coordinates, Zone Classifications, and Dominant Emission Sources.

Station Name	Code	Latitude	Longitude	Zone Classification	Primary VOC Emission Drivers
Ballygunge	BG	22.5264°N	88.3692°E	Residential/Commercial	High-density vehicular traffic, domestic fuel, commercial solvents
Barrackpore	SVSPA	22.7661°N	88.3644°E	Industrial/Suburban	Paper mills, textile printing, suburban arterial freight corridor
Belur Math	BM	22.6362°N	88.3521°E	Religious/Riverbank	Ferry diesel exhaust, Grand Trunk Road vehicular traffic, rail idling
Bidhannagar	BN	22.5802°N	88.4331°E	Commercial/IT Park	IT transit fleet, architectural coating solvents, commercial diesel generators
Botanical Garden	BOG	22.5473°N	88.2941°E	Green Background	River-borne advection of industrial foundry plumes from adjacent Howrah belt
Dasnagar	DN	22.5921°N	88.3053°E	Heavy Industrial	Metal casting foundries, rolling mills, chemical plants, solvent evaporation
Fort William	FW	22.5532°N	88.3444°E	Semi-Urban/Parkland	Military cantonment transit, central Maidan buffer, arterial perimeter transit
Ghusuri	GH	22.5824°N	88.3163°E	Heavy Industrial	Glass furnaces, steel foundries, diesel freight terminals, chemical storage
Jadavpur	JD	22.4991°N	88.3713°E	Mixed Urban/Traffic	Small-scale engineering workshops, intense stop-and-go vehicular exhaust
Padmapukur	PP	22.5651°N	88.3072°E	Industrial/Residential	Water treatment chlorination, localized foundries, Kona Expressway freight
Rabindra Bharati Univ	RBU	22.5932°N	88.3724°E	Traffic Hotspot	High-density arterial junction (BT Road), heavy vehicle braking and idling
Rabindra Sarovar	RS	22.5083°N	88.3582°E	Urban Park	Lake water-body buffer, perimeter Southern Avenue vehicular road network
Victoria Memorial	VC	22.5441°N	88.3432°E	Urban Background	Heritage parkland green buffer, perimeter tourism transit, central river breeze

2.2 Analytical Instrumentation and QA/QC Protocols

Ambient monoaromatic hydrocarbons were quantified using automated online gas chromatographs equipped with photoionization detectors (Synspec GC955, Synspec B.V., Groningen, Netherlands) installed inside climate-controlled monitoring shelters (20–25°C). The instrument operates on a continuous 15-minute cycle (96 sampling and analytical cycles per 24-hour period). Ambient air is sampled through an inert polytetrafluoroethylene (PTFE) sampling line fitted with a $2\,\mu$m particulate pre-filter. Sample air is continuously drawn across an internal Tenax adsorbent pre-concentrator maintained at ambient shelter temperature. Following pre-concentration, the adsorbent trap undergoes rapid thermal desorption (250°C), injecting the concentrated organic pulse onto a capillary separation column (AT-5 or DB-1 equivalent, $30\text{ m} \times 0.32$ mm inner diameter).

Component separation is achieved isothermally with nitrogen (N_2, 99.999% purity) as the carrier gas. Eluting hydrocarbon species pass into a photoionization detector utilizing a high-intensity krypton discharge lamp emitting ultraviolet photons at 10.6 eV. Photons ionize target monoaromatic molecules possessing ionization potentials below 10.6 eV (Benzene: 9.24 eV; Toluene: 8.82 eV; Ethylbenzene: 8.77 eV; *o*-Xylene: 8.56 eV; *m*-Xylene: 8.56 eV; *p*-Xylene: 8.44 eV), while avoiding ionization of major atmospheric bulk gases (N_2: 15.58 eV; O_2: 12.07 eV; CO_2: 13.78 eV; methane: 12.61 eV). Produced ion currents are amplified and converted to digital chromatographic area counts.

Detection limits for individual BTEX species are $0.10\,\mu$g m^{-3} for benzene, $0.10\,\mu$g m^{-3} for toluene, and $0.15\,\mu$g m^{-3} for ethylbenzene and xylene isomers. Precision and accuracy evaluated through duplicate injections demonstrate relative standard deviations (RSD) below 5%. Quality assurance protocols enforced automated zero-air baseline compensation every 24 hours and weekly multipoint span gas calibrations using NIST-traceable certified gas standards (5-component BTEX calibration mixture in balance nitrogen, Air Liquide / Linde). Co-located meteorological variables—including horizontal wind speed (WS, m s^{-1}), horizontal wind direction (WD, degrees from True North), ambient air temperature (AT, °C), relative humidity (RH, %), and solar radiation (SR, W m^{-2})—were recorded simultaneously using Met One Instruments 2D sonic anemometers and meteorological sensor packages mounted on 10 m mast towers adjacent to station shelter roofs.

2.3 Definition of Total Measured VOCs ($\sum$BTEX)

In this empirical monitoring dataset, total measured volatile organic compound concentration (VOC_{Total}) is strictly defined as the stoichiometric mass sum of the five measured monoaromatic BTEX species:

$$VOC_{Total} \equiv \sum BTEX = C_{Benzene} + C_{Toluene} + C_{Ethylbenzene} + C_{m,p\text{-}Xylene} + C_{o\text{-}Xylene} \quad (5)$$

This mathematical equality was verified across all 26 station-year primary telemetry workbooks covering 721,193 individual observations; the maximum absolute residual observed between recorded VOC_{Total} and the component sum was $< 5.68 \times 10^{-14}\,\mu$g m^{-3}, confirming machine-precision closure. Non-aromatic VOC classes (aliphatic alkanes, alkenes, biogenic terpenes, and carbonyls) were not quantified by the online gas chromatography systems. Therefore, all total VOC metrics reported herein represent speciated monoaromatic loading ($\sum$BTEX) rather than total non-methane organic carbon.

2.4 Mathematical Formulation of the Conditional Probability Function (CPF)

The Conditional Probability Function (CPF) evaluates the probability that an observed concentration from a designated horizontal wind direction sector exceeds a specified upper-percentile threshold (Ashbaugh et al., 1985; Zhang et al., 2014):

$$\mathrm{CPF}_{\Delta\theta} = \left.\frac{m_{\Delta\theta}}{n_{\Delta\theta}}\right|_{C>\tau} \tag{6}$$

where $n_{\Delta\theta}$ is the total number of valid observations within wind direction sector $\Delta\theta$, $m_{\Delta\theta}$ is the number of observations within sector $\Delta\theta$ for which the measured pollutant concentration or diagnostic ratio C exceeds a predefined threshold τ, and $\Delta\theta$ denotes the sector bin width.

In this investigation, parameters were established following standardized micrometeorological criteria:

1. Calm Wind Screening: Light wind conditions ($\mathrm{WS} \leq 0.5$ m s^{-1}) were screened from directional CPF computation. Under calm conditions, mechanical cup and vane friction thresholds and thermal turbulence render anemometer wind direction readings non-vectorial and unstable, preventing meaningful source orientation.

2. Sector Discretization: Wind azimuth was discretized into 36 equal sectors of $\Delta\theta = 10^\circ$, spanning from 0° to 360° clockwise from True North.

3. Threshold Selection: The concentration threshold was set to the 90th percentile ($\tau = P_{90}$) calculated across the entire valid continuous time series for that station and pollutant, isolating the top decile of extreme emission events.

4. Circular Smoothing: To minimize statistical noise arising from discrete sector transitions while preserving true peak orientations, raw CPF distributions were smoothed using a three-point circular moving average:

$$\widetilde{\mathrm{CPF}}_i = \frac{1}{3}\sum_{k=-1}^{1} \mathrm{CPF}_{(i+k) \bmod 36} \tag{7}$$

5. Coordinate Conventions: Polar plots follow standard meteorological conventions: 0° = North (top), 90° = East (right), 180° = South (bottom), and 270° = West (left). The recorded wind direction θ indicates the direction from which the wind is blowing. Consequently, an elevated CPF probability lobe aligned toward 270° indicates that air parcels originating from the west transport pollutant concentrations in excess of the 90th percentile.

2.5 Photochemical Reactivity and Ozone Formation Potential (OFP) Models

The photochemical contribution of individual monoaromatics to tropospheric ozone formation was evaluated using the Maximum Incremental Reactivity (MIR) method developed by Carter (Carter, 1994, 2010):

$$\mathrm{OFP}_i = [\mathrm{VOC}]_i \times \mathrm{MIR}_i \tag{8}$$

$$\mathrm{OFP}_{\mathrm{Total}} = \sum_{i=1}^{5} \mathrm{OFP}_i \tag{9}$$

where $[\mathrm{VOC}]_i$ is the mass concentration of species i (μg m^{-3}) and MIR_i is the dimensionless Maximum Incremental Reactivity coefficient (g O_3/g VOC) representing the grams of ozone produced per gram of VOC added to a reference photochemical atmosphere under conditions where ozone formation is highly sensitive to VOCs. The updated SAPRC-07 chemical mechanism MIR coefficients were applied (Carter, 2010): Benzene = 0.72, Toluene = 3.97, Ethylbenzene = 2.70, *m*, *p*-Xylene = 9.75, and *o*-Xylene = 7.49.

To assess relative photochemical consumption rates, the mass-weighted OH kinetic reactivity index ($R_{\mathrm{OH},i}$, μg m^{-3} cm^3 molecule^{-1} s^{-1}) and propene-equivalent concentration (Pro-Equiv$_i$, μg m^{-3}) were calculated (Chameides et al., 1992; Atkinson and Arey, 2003):

$$R_{\mathrm{OH},i} = k_{\mathrm{OH},i} \times [\mathrm{VOC}]_i \tag{10}$$

$$\text{Pro-Equiv}_i = [\mathrm{VOC}]_i \times \frac{k_{\mathrm{OH},i}}{k_{\mathrm{OH,propene}}} \tag{11}$$

Second-order reaction rate constants with OH radicals at 298 K (k_{OH}, in units of 10^{-12} cm^3 molecule^{-1} s^{-1}) were obtained from evaluated chemical kinetics literature (Atkinson and Arey, 2003): Benzene = 1.22, Toluene = 5.63, Ethylbenzene = 7.00, *m*, *p*-Xylene = 23.60, *o*-Xylene = 13.60, and Propene reference = 26.30.

2.6 Quantitative Inhalation Carcinogenic and Non-Carcinogenic Health Risk Assessment

2.6.1 Concentration-Based Inhalation Unit Risk Framework (WHO & USEPA RAGS Part F / IRIS)

In accordance with contemporary USEPA inhalation dosimetry guidance (Risk Assessment Guidance for Superfund, RAGS Part F) (USEPA, 2009) and World Health Organization guidelines (WHO, 2000, 2010), chronic carcinogenic risk from the inhalation of volatile organic compounds is quantified directly through concentration-based unit risk

metrics:

$$\mathrm{ILCR} = \mathrm{IUR} \times C_{\mathrm{air}} \tag{12}$$

where C_{air} is the ambient benzene concentration (μg m^{-3}) under continuous lifetime exposure, and IUR is the chemical-specific Inhalation Unit Risk ((μg m^{-3})$^{-1}$). This concentration-based framework directly avoids unwarranted extrapolations of reference adult body weight (e.g., 70 kg vs 60 kg) and daily volumetric inhalation rates (20 m^3 day^{-1}) that characterized legacy intake-dose models (RAGS Part A) (USEPA, 1989).

We evaluate two authoritative, peer-reviewed concentration-based benchmarks:

1. WHO Inhalation Unit Risk: $\mathrm{IUR}_{\mathrm{WHO}} = 6.0 \times 10^{-6}\,(\mu\mathrm{g\ m^{-3}})^{-1}$ for lifetime excess leukemia risk, established in the WHO Air Quality Guidelines for Europe (WHO, 2000) and reaffirmed in WHO indoor air quality guidelines (WHO, 2010) (the 2021 WHO Global Air Quality Guidelines focused exclusively on criteria pollutants and did not re-evaluate hazardous air pollutants or chemical carcinogens):

$$\mathrm{ILCR}_{\mathrm{WHO}} = C_{\mathrm{air}} \times 6.0 \times 10^{-6} \tag{13}$$

2. USEPA IRIS Inhalation Unit Risk Range and Midpoint: The USEPA Integrated Risk Information System (IRIS) toxicological review (USEPA, 2000) establishes an Inhalation Unit Risk range of $\mathrm{IUR}_{\mathrm{IRIS}} = (2.2\text{–}7.8) \times 10^{-6}\,(\mu\mathrm{g\ m^{-3}})^{-1}$ based on human occupational leukemia cohorts. Because the IRIS assessment presents this uncertainty range without designating a single central point estimate, we report the arithmetic midpoint of the range, $\mathrm{IUR}_{\mathrm{IRIS,\ midpoint}} = 5.0 \times 10^{-6}\,(\mu\mathrm{g\ m^{-3}})^{-1}$ (i.e., $[2.2+7.8]/2 \times 10^{-6}$), as a standardized screening point estimate, alongside the full range for sensitivity bounds:

$$\mathrm{ILCR}_{\mathrm{IRIS,\ midpoint}} = C_{\mathrm{air}} \times 5.0 \times 10^{-6} \quad \left[\text{Uncertainty Range: } C_{\mathrm{air}} \times (2.2\text{–}7.8) \times 10^{-6}\right] \tag{14}$$

Regulatory screening benchmarks define $\mathrm{ILCR} < 1 \times 10^{-6}$ (one in a million excess lifetime cancer cases) as the negligible (de minimis) risk threshold. Risks between 1×10^{-6} and 1×10^{-4} denote an actionable regulatory range warranting monitoring and mitigation, while risks exceeding 1×10^{-4} (100×10^{-6}) denote an intolerable lifetime health risk requiring urgent emission controls (WHO, 2000, 2010; USEPA, 2009).

For comparison with historical South Asian literature applying legacy dose-intake equations (USEPA, 1989), an adult continuous intake model using the legacy USEPA HEAST (1997) Inhalation Slope Factor ($\mathrm{CSF} = 0.029\,(\mathrm{mg\ kg^{-1}\ day^{-1}})^{-1}$) (USEPA, 1997; Rinsky et al., 1987) corresponds to an effective conversion factor of $8.29 \times 10^{-6}\,(\mu\mathrm{g\ m^{-3}})^{-1}$. This legacy intake metric produces results of the same magnitude as the WHO unit-risk benchmark and falls within the USEPA IRIS upper uncertainty bounds, confirming

that all standard evaluation frameworks identify pronounced carcinogenic risk across the conurbation.

2.6.2 Chronic Non-Carcinogenic Hazard Quotient

Chronic non-carcinogenic respiratory and hematological risk is evaluated using the Hazard Quotient (HQ) relative to the chronic Inhalation Reference Concentration ($\mathrm{RfC} = 30\,\mu\mathrm{g\ m^{-3}}$) established by the USEPA (USEPA, 2000):

$$\mathrm{HQ} = \frac{C_{\mathrm{air}}}{\mathrm{RfC}} = \frac{C_{\mathrm{air}}}{30.0\,\mu\mathrm{g\ m^{-3}}} \tag{15}$$

An $\mathrm{HQ} \leq 1.0$ indicates that ambient exposure remains below the threshold for chronic non-carcinogenic toxic effects.

2.7 Statutory Benchmark: Indian CPCB NAAQS and Data Completeness

India's mandatory statutory National Ambient Air Quality Standard (NAAQS) for Benzene (CPCB Notification No. B-29016/20/90/PCI-L, dated 18 November 2009) sets the annual arithmetic average limit at:

$$\mathrm{NAAQS}_{\mathrm{Benzene}} = 5.0\,\mu\mathrm{g\ m^{-3}} \tag{16}$$

Under CPCB and USEPA 40 CFR Part 58 regulatory guidelines, a statistically valid annual average requires at least 75% valid data capture across each calendar quarter. Where this completeness threshold is satisfied, observed means exceeding $5.0\,\mu\mathrm{g\ m^{-3}}$ constitute a breach of the statutory environmental benchmark. Where temporal coverage fails the 75% criterion, observed values are reported as seasonal averages and qualified accordingly. Computational Framework and AI Disclosure: All data processing, statistical modeling, and validation pipelines were implemented in Python 3.13. Generative AI tools (Anthropic Claude and Google Gemini) assisted substantially in computational script development, mathematical formalization, structuration of theoretical linkages, and manuscript drafting and language editing. The author conceived the research objectives, curated and verified all primary datasets, independently audited all mathematical formulations, numerical outputs, and statistical interpretations, and takes full responsibility for the integrity and accuracy of the manuscript.

3 Results

3.1 Spatiotemporal BTEX Speciation Profiles (2024 vs 2025)

Tables 2 and 3 present the annual arithmetic mean concentrations of speciated BTEX compounds, total measured monoaromatic sum ($\sum$BTEX), diagnostic T/B ratios, CPCB statutory compliance status, and inhalation cancer risk metrics for all 13 CAAQMS stations during calendar years 2024 and 2025. Speciated columns for Ethylbenzene, *m*, *p*-Xylene, and *o*-Xylene reflect verified empirical telemetry.

Table 2. Annual Mean (μg m^{-3}) BTEX Concentrations, Monoaromatic Sum ($\sum$BTEX), T/B Ratios, CPCB NAAQS Compliance, and Inhalation Cancer Risks across all 13 CAAQMS Stations (2024).

Station Name	Benzene	Toluene	Eth-Benz	*mp*-Xyl	*o*-Xyl	$\sum$BTEX	T/B	NAAQS[a] (5.0)	HQ	ILCR$_{\text{WHO}}$ ($\times 10^{-6}$)	ILCR$_{\text{IRIS}}$ ($\times 10^{-6}$)
Jadavpur	18.07	8.53	1.46	1.84	0.98	30.89	0.47	Exceeded	0.60	108.43	90.35
Botanical Garden[b]	9.63	15.90	7.42	0.93	0.64	34.52	1.65	(Exceeded)	0.32	57.81	48.15
Dasnagar[c]	7.44	14.41	6.73	7.77	3.68	40.03	1.94	(Exceeded)	0.25	44.64	37.20
Ballygunge	6.33	8.12	1.44	2.29	1.24	19.42	1.28	Exceeded	0.21	37.98	31.65
Belur Math	5.33	4.83	0.51	0.77	0.71	12.15	0.91	Exceeded	0.18	31.95	26.65
Padmapukur	5.11	6.98	2.29	3.63	1.71	19.71	1.37	Exceeded	0.17	30.64	25.55
Rabindra Sarovar	4.37	5.51	1.02	1.46	0.78	13.14	1.26	Compliant	0.15	26.25	21.85
Rabindra Bharati Univ	4.11	9.15	2.02	1.27	0.61	17.16	2.23	Compliant	0.14	24.66	20.55
Victoria Memorial	4.03	4.99	1.00	1.16	0.57	11.75	1.24	Compliant	0.13	24.20	20.15
Ghusuri	2.68	9.55	1.72	3.72	1.50	19.17	3.56	Compliant	0.09	16.08	13.40
Bidhannagar	2.43	4.81	0.76	1.07	0.54	9.59	1.98	Compliant	0.08	14.56	12.15
Fort William	2.24	3.19	1.15	1.02	0.42	8.02	1.42	Compliant	0.07	13.45	11.20
Barrackpore (SVSPA)[d]	1.49	4.77	1.84	1.94	0.91	10.95	3.20	Compliant	0.05	8.94	7.45

[a] CPCB NAAQS statutory annual standard for Benzene is 5.0 μg m^{-3}. Parentheses indicate seasonal exceedance where annual completeness was $< 75\%$.
[b] Botanical Garden 2024 monitored from June 14 to November 23 (13,745 rows, 39.12% capture; missing peak winter Jan–Feb and Dec).
[c] Dasnagar 2024 monitored from October 15 to December 31 (6,843 rows, 19.48% capture; peak winter smog window only).
[d] Barrackpore (SVSPA) 2024 monitored from March 29 to December 31 (20,024 rows, 56.99% capture; missing Q1).
Note: ILCR$_{\text{WHO}}$ and ILCR$_{\text{IRIS}}$ evaluate concentration-based Inhalation Unit Risk ($\text{ILCR} = \text{IUR} \times C_{\text{air}}$) using WHO ($6.0 \times 10^{-6}$ (μg m^{-3})$^{-1}$; WHO 2000, 2010) and USEPA IRIS midpoint (5.0×10^{-6} (μg m^{-3})$^{-1}$, representing the arithmetic midpoint of the IRIS uncertainty range of 2.2–7.8×10^{-6}; USEPA 2000) benchmarks. Under legacy intake-dose models (HEAST 1997 $SF_i = 0.029$), Jadavpur evaluates to 149.73×10^{-6}.

In 2024, total monoaromatic loading ($\sum$BTEX) among stations with complete annual coverage ranged from 8.02 μg m^{-3} at Fort William to 30.89 μg m^{-3} at Jadavpur. At the heavy industrial site of Dasnagar, where monitoring in 2024 was restricted to the post-monsoon and winter seasons, $\sum$BTEX reached 40.03 μg m^{-3}. In 2025, network-wide $\sum$BTEX averaged between 6.36 μg m^{-3} at Victoria Memorial and 34.05 μg m^{-3} at Botanical Garden, with Jadavpur recording 28.15 μg m^{-3}. Across both monitoring years, toluene and benzene represented the two most abundant species, jointly accounting for 58%–85% of total monoaromatic mass across all stations.

Table 3. Annual Mean (μg m^{-3}) BTEX Concentrations, Monoaromatic Sum ($\sum$BTEX), T/B Ratios, CPCB NAAQS Compliance, and Inhalation Cancer Risks across all 13 CAAQMS Stations (2025).

Station Name	Benzene	Toluene	Eth-Benz	*mp*-Xyl	*o*-Xyl	$\sum$BTEX	T/B	NAAQS[a] (5.0)	HQ	ILCR$_{WHO}$ ($\times 10^{-6}$)	ILCR$_{IRIS}$ ($\times 10^{-6}$)
Jadavpur	14.61	9.16	1.48	1.85	1.06	28.15	0.63	Exceeded	0.49	87.65	73.05
Botanical Garden	8.29	12.50	6.50	4.51	2.26	34.05	1.51	Exceeded	0.28	49.76	41.45
Ballygunge	4.83	6.95	1.81	2.44	1.47	17.51	1.44	Compliant	0.16	29.01	24.15
Padmapukur[f]	4.21	3.19	1.24	1.57	0.93	11.14	0.76	Not assessable[a]	0.14	25.23	21.05
Belur Math	4.17	3.88	0.50	1.20	0.79	10.55	0.93	Compliant	0.14	25.01	20.85
Rabindra Sarovar	3.78	4.78	1.18	1.27	0.75	11.76	1.27	Compliant	0.13	22.66	18.90
Rabindra Bharati Univ	3.12	7.41	1.45	1.24	0.60	13.81	2.38	Compliant	0.10	18.70	15.60
Barrackpore (SVSPA)	2.80	7.42	1.34	2.99	0.70	15.24	2.65	Compliant	0.09	16.79	14.00
Ghusuri	2.77	4.52	0.90	2.45	0.73	11.37	1.63	Compliant	0.09	16.64	13.85
Dasnagar	2.71	5.02	2.91	3.22	1.43	15.30	1.86	Compliant	0.09	16.24	13.55
Fort William[e]	2.64	4.52	1.32	1.23	0.66	10.38	1.71	Not assessable[a]	0.09	15.86	13.20
Bidhannagar	1.80	4.43	0.59	0.85	0.38	8.05	2.45	Compliant	0.06	10.83	9.00
Victoria Memorial	1.70	2.38	1.06	0.71	0.51	6.36	1.40	Compliant	0.06	10.17	8.50

[a] CPCB NAAQS statutory annual standard for Benzene is 5.0 μg m^{-3}. Stations failing the $\geq 75\%$ quarterly completeness threshold are designated as Not Assessable for formal statutory annual compliance under CPCB and USEPA 40 CFR Part 58 regulatory criteria.
[e] Fort William in 2025 recorded 19,917 observations (56.84% capture) due to an extended monitoring gap between May 20 and July 24, 2025 (65 days); designated as not assessable for annual compliance under the 75% quarterly criterion.
[f] Padmapukur in 2025 recorded 26,077 observations (74.42% capture) due to an extended monitoring gap between July 25 and September 13, 2025 (50 days); designated as not assessable for annual compliance under the 75% quarterly criterion.
Note: ILCR$_{WHO}$ and ILCR$_{IRIS}$ evaluate concentration-based Inhalation Unit Risk ($ILCR = IUR \times C_{air}$) using WHO ($6.0 \times 10^{-6}$ (μg m^{-3})$^{-1}$; WHO 2000, 2010) and USEPA IRIS midpoint (5.0×10^{-6} (μg m^{-3})$^{-1}$, representing the arithmetic midpoint of the IRIS uncertainty range of 2.2–7.8 $\times 10^{-6}$; USEPA 2000) benchmarks.

3.2 Observational Completeness and Seasonal Sensitivity Analysis

A prominent observation between 2024 and 2025 is the apparent decline in recorded annual $\sum$BTEX at Dasnagar from $40.03\,\mu$g m^{-3} to $15.30\,\mu$g m^{-3} (a nominal -61.8% reduction). Detailed examination of the raw telemetry records reveals that this difference is an artifact of seasonal sampling bias rather than inter-annual emission moderation.

At Dasnagar, the monitoring station was commissioned on October 15, 2024. Consequently, calendar year 2024 captured only 6,843 valid 15-minute observations (19.48% annual data capture), representing exclusively the severe post-monsoon and winter pollution window (October 15 to December 31). In the lower Gangetic plain, winter meteorology is characterized by strong nocturnal radiation inversions, suppressed boundary-layer mixing depths (< 150–200 m), and stagnant surface winds, which trap localized foundry and metal casting emissions. Conversely, in 2025, Dasnagar operated across the full annual meteorological cycle (27,328 observations, 77.99% data capture), encompassing the pre-monsoon and monsoon seasons where intense precipitation washout and deep convective planetary boundary layers ($> 1,500$ m) disperse atmospheric trace gases. During the 2025 monsoon (July–September), Dasnagar mean benzene concentration dropped to $0.07\,\mu$g m^{-3} and $\sum$BTEX dropped to $0.72\,\mu$g m^{-3}.

To establish a valid inter-annual comparison, we restricted both datasets to the identical calendar window (October 15 to December 31):

- In 2024 (Oct 15–Dec 31): Dasnagar mean benzene was $7.44\,\mu$g m^{-3} and $\sum$BTEX was $40.03\,\mu$g m^{-3}.
- In 2025 (Oct 15–Dec 31): Dasnagar mean benzene was $5.55\,\mu$g m^{-3} and $\sum$BTEX was $34.17\,\mu$g m^{-3}.

Comparing identical calendar periods reveals that winter benzene altered by -25.4% and $\sum$BTEX altered by -14.7%, confirming that localized industrial activity remained persistent, with the apparent 61.8% annual collapse driven by seasonal temporal dilution in the full-year 2025 record.

Similar seasonal constraints influenced Botanical Garden in 2024 (39.12% capture, unmonitored during the peak winter months of January–February and December) and Barrackpore SVSPA in 2024 (56.99% capture, unmonitored during Q1 winter). Conversely, at stations with complete continuous capture in both years ($> 85\%$), such as Jadavpur (89.30% in 2024; 93.43% in 2025) and Ballygunge (91.12% in 2024; 94.20% in 2025), annual benzene concentrations declined from 18.07 to $14.61\,\mu$g m^{-3} (-19.2%) and from 6.33 to $4.83\,\mu$g m^{-3} (-23.7%), respectively, reflecting legitimate network trends.

3.3 Diagnostic Emission Ratios and Chemical Fingerprinting

The spatial distribution of Toluene-to-Benzene (T/B) mass ratios reveals distinct chemical emission regimes across the metropolitan conurbation:

1. Vehicular Combustion Regimes ($T/B \leq 1.0$): Documented at Jadavpur (0.47 in 2024; 0.63 in 2025), Belur Math (0.91 in 2024; 0.93 in 2025), and Padmapukur (0.76 in 2025). High benzene relative to toluene reflects unburned fuel exhaust, cold-start vehicular emissions, and stop-and-go driving patterns in congested street canyons.

2. Mixed Urban Transit Regimes ($1.0 < T/B \leq 1.5$): Observed at Ballygunge (1.28 in 2024; 1.44 in 2025), Rabindra Sarovar (1.26 in 2024; 1.27 in 2025), Victoria Memorial (1.24 in 2024; 1.40 in 2025), and Fort William (1.42 in 2024; 1.71 in 2025), reflecting blended contributions from mixed vehicular fleets and commercial solvents.

3. Industrial Solvent Evaporation Regimes ($T/B > 1.5$): Highly prominent at Ghusuri (3.56 in 2024; 1.63 in 2025), Barrackpore SVSPA (3.20 in 2024; 2.65 in 2025), Rabindra Bharati University (2.23 in 2024; 2.38 in 2025), Dasnagar (1.94 in 2024; 1.86 in 2025), and Botanical Garden (1.65 in 2024; 1.51 in 2025). The marked elevation in toluene fingerprints heavy localized emissions from paint formulations, polymer curing, metal degreasing, and chemical solvent handling in the Howrah and northern industrial belts.

3.4 Photochemical Reactivity and Ozone Formation Potential (OFP) Dynamics

Table 4 summarizes the calculated Ozone Formation Potential (OFP_{Total}), species-specific percentage contributions, propene-equivalent concentrations (Pro-Equiv), and mass-weighted OH kinetic reactivity indices (R_{OH}) across all 13 stations for both years.

A primary scientific insight emerges from comparing species mass fractions with their photochemical reactivity. In 2024, total OFP ranged from $30.47\,\mu g\ m^{-3}$ at Fort William to $184.06\,\mu g\ m^{-3}$ during the Dasnagar winter window. Although Benzene dominates the carcinogenic risk profile, it contributes on average only 6.2% of network-wide OFP (ranging from 2.1% at Ghusuri and SVSPA to 17.1% at Jadavpur) due to its low MIR coefficient (0.72).

In contrast, Toluene accounts on average for 45.3% of network OFP (peaking at 60.7% at Botanical Garden and 58.9% at RBU). Xylene isomers (m,p-Xylene and o-Xylene), despite existing at lower ambient mass concentrations than benzene, contribute on average 40.7% of network OFP (reaching 56.1% at Dasnagar, 56.2% at Padmapukur, and 51.6%

Table 4. Calculated Ozone Formation Potential (OFP) and Photochemical Reactivity Metrics across all 13 CAAQMS Stations for 2024 and 2025 using Carter Maximum Incremental Reactivity (MIR) Coefficients.

Station Name	2024 Photochemical Reactivity						2025 Photochemical Reactivity					
	OFP_{Tot} (μg m^{-3})	%B	%T	%Xyl	Pro-Eq (μg m^{-3})	R_{OH} (*)	OFP_{Tot} (μg m^{-3})	%B	%T	%Xyl	Pro-Eq (μg m^{-3})	R_{OH} (*)
Jadavpur	76.10	17.1%	44.5%	33.2%	5.21	1.4×10^{-10}	76.86	13.7%	47.3%	33.8%	5.24	1.4×10^{-10}
Botanical Garden	103.95	6.7%	60.7%	13.3%	6.99	1.8×10^{-10}	134.04	4.5%	37.0%	45.4%	10.01	2.6×10^{-10}
Dasnagar	184.06	2.9%	31.1%	56.1%	14.10	3.7×10^{-10}	71.84	2.7%	27.7%	58.6%	5.60	1.5×10^{-10}
Ballygunge	72.30	6.3%	44.6%	43.7%	5.11	1.3×10^{-10}	70.76	4.9%	39.0%	49.2%	5.14	1.4×10^{-10}
Belur Math	37.22	10.3%	51.5%	34.5%	2.48	6.5×10^{-11}	37.37	8.0%	41.2%	47.1%	2.64	6.9×10^{-11}
Padmapukur	85.77	4.3%	32.3%	56.2%	6.48	1.7×10^{-10}	41.32	7.3%	30.7%	53.9%	3.10	8.1×10^{-11}
Rabindra Sarovar	47.85	6.6%	45.7%	42.0%	3.37	8.9×10^{-11}	42.88	6.3%	44.3%	42.0%	3.04	8.0×10^{-11}
Rabindra Bharati Univ	61.69	4.8%	58.9%	27.5%	4.14	1.1×10^{-10}	52.16	4.3%	56.4%	31.8%	3.54	9.3×10^{-11}
Victoria Memorial	40.99	7.1%	48.3%	38.0%	2.86	7.5×10^{-11}	24.28	5.0%	38.9%	44.2%	1.77	4.7×10^{-11}
Ghusuri	91.99	2.1%	41.2%	51.6%	6.74	1.8×10^{-10}	51.72	3.9%	34.7%	56.8%	3.91	1.0×10^{-10}
Bidhannagar	37.37	4.7%	51.1%	38.7%	2.58	6.8×10^{-11}	31.61	4.1%	55.6%	35.2%	2.15	5.6×10^{-11}
Fort William	30.47	5.3%	41.6%	43.0%	2.23	5.9×10^{-11}	40.35	4.7%	44.5%	42.0%	2.89	7.6×10^{-11}
Barrackpore (SVSPA)	50.71	2.1%	37.3%	50.7%	3.79	1.0×10^{-10}	69.49	2.9%	42.4%	49.5%	5.12	1.3×10^{-10}

*Mass-weighted OH kinetic reactivity index R_{OH} in units of μg m^{-3} cm^3 molecule^{-1} s^{-1}. Note: MIR coefficients (Carter, 2010): Benzene = 0.72, Toluene = 3.97, Ethylbenzene = 2.70, *m*, *p*-Xylene = 9.75, *o*-Xylene = 7.49 g O_3/g VOC. Rate constants k_{OH} at 298 K ($\times10^{-12}$ cm^3 molecule^{-1} s^{-1}): Benzene = 1.22, Toluene = 5.63, Ethylbenzene = 7.00, *m*, *p*-Xylene = 23.60, *o*-Xylene = 13.60, Propene reference = 26.30. %Xyl denotes combined (*m*, *p*-Xylene + *o*-Xylene) contribution to total OFP.

at Ghusuri) owing to the high MIR value of *m*, *p*-xylene (9.75) and its rapid OH radical reaction rate (23.6×10^{-12} cm^3 molecule^{-1} s^{-1}). Together, Toluene and Xylenes account for $>85\%$ of total secondary ozone production capacity across the entire conurbation. Propene-equivalent concentrations (Pro-Equiv) exhibited a six-fold gradient, ranging from 2.23 μg m^{-3} at Fort William to 14.10 μg m^{-3} at Dasnagar in 2024, and from 1.77 μg m^{-3} at Victoria Memorial to 10.01 μg m^{-3} at Botanical Garden in 2025.

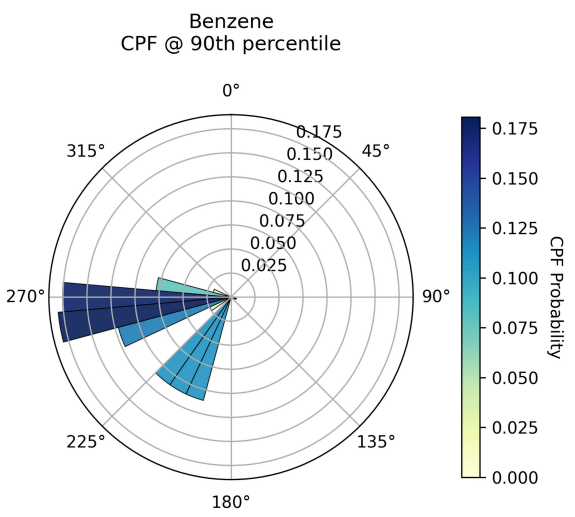
3.5 Directional Source Identification via Conditional Probability Functions (CPF)

3.5.1 Directional Benzene Transport Corridors

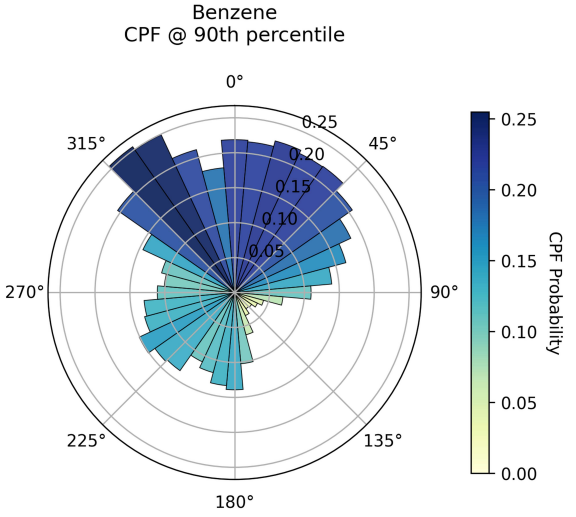
Figure 2 illustrates Conditional Probability Function (CPF) polar plots for Benzene at the 90th percentile threshold (P_{90}) across four contrasting urban microclimates: Jadavpur (vehicular hotspot), Ghusuri (heavy industrial), Dasnagar (metal casting), and Victoria Memorial (urban background).

The polar vectors demonstrate pronounced land-use-specific directional signatures:

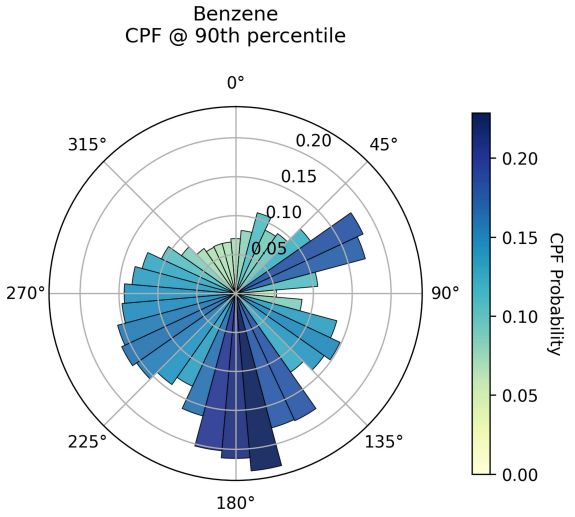
1. Jadavpur (Figure 2a): The CPF distribution exhibits radial dispersion with prominent probability lobes extending toward the south and southwest (180°–230°). This pattern fingerprints localized ground-level mobile emissions from the major Prince Anwar Shah Road and Raja S.C. Mullick Road intersections, where stop-and-go



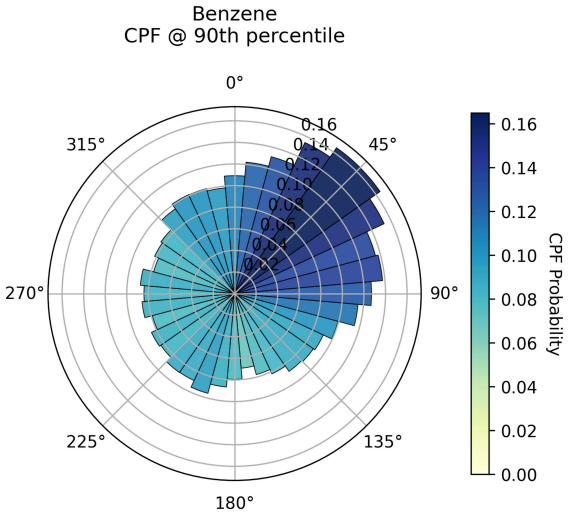
(a) Jadavpur (Vehicular Hotspot / Cancer Peak)



(b) Ghusuri (Heavy Industrial Foundries)



(c) Dasnagar (Metal Casting Cluster)



(d) Victoria Memorial (Urban Background)

Fig. 2 Conditional Probability Function (CPF) polar plots for Benzene (90th percentile threshold) across four contrasting microclimates in Kolkata and Howrah

driving, idling auto-rickshaw stands, and cold-start vehicular exhaust produce high benzene loadings independent of wind speed.

2. Ghusuri (Figure 2b): Shows dominant, elongated probability lobes oriented toward the west and northwest (280°–320°). Under moderate-to-high westerly wind speeds (> 2.5 m s^{-1}), high-concentration benzene plumes are advected directly from metallurgical re-rolling mills, galvanizing units, and coal-fired foundries located along the Howrah industrial corridor.

3. Dasnagar (Figure 2c): Displays broad westerly and south-westerly lobes (220°–270°), pointing toward the dense cluster of iron foundries, engineering casting facilities, and paint workshops situated along the Baltikuri and Shanpur industrial zones.

4. Victoria Memorial (Figure 2d): Located in central Kolkata parkland, Victoria Memorial exhibits substantially lower absolute CPF probability (< 0.25), with subtle lobes pointing north-northeast (0°–30°), capturing regional winter drainage channeling down the Hooghly River valley from northern industrial belts.

3.5.2 Diagnostic T/B Ratio Polar Corridors

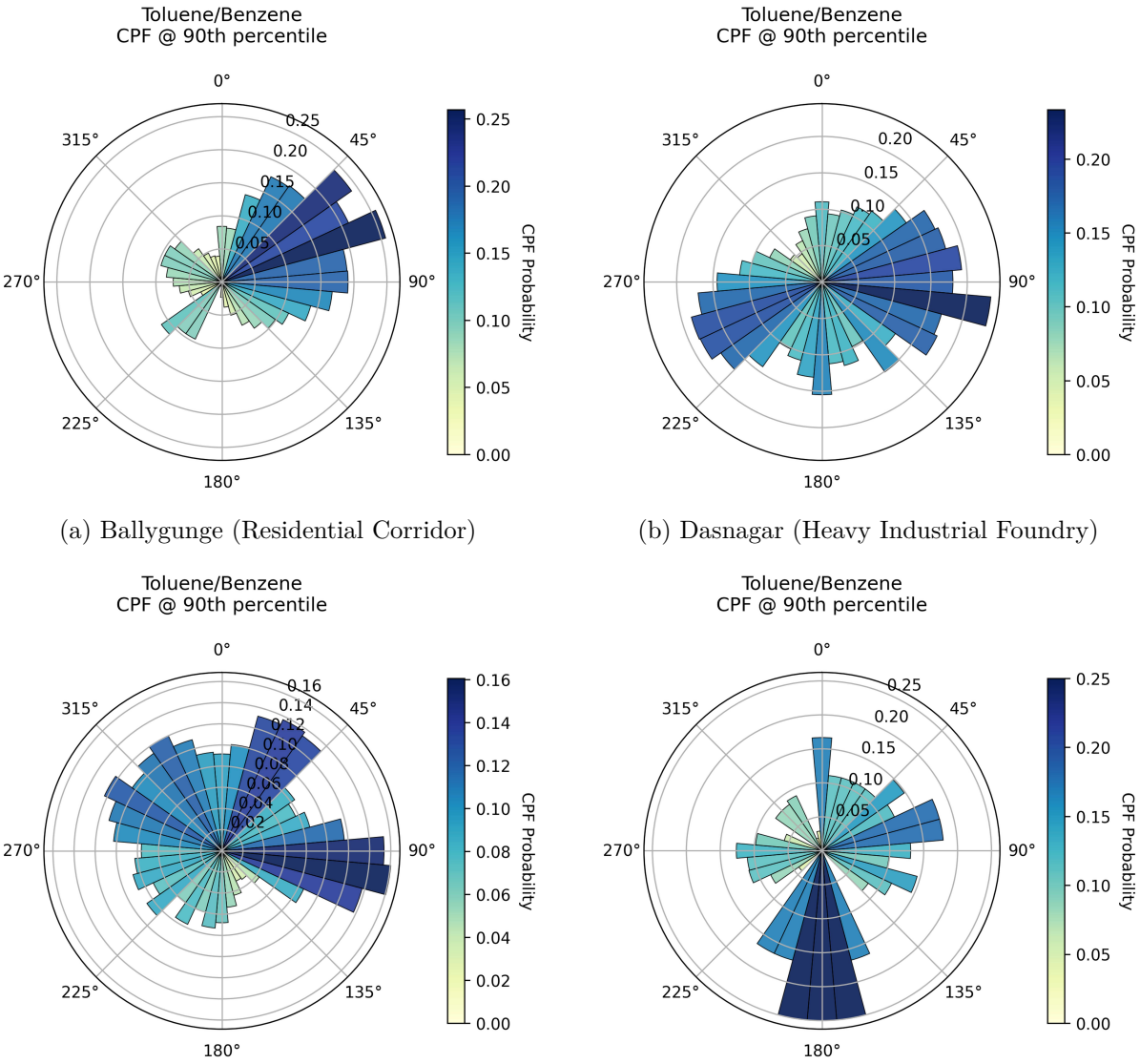
Figure 3 presents CPF polar plots for the Toluene-to-Benzene (T/B) diagnostic ratio across Ballygunge, Dasnagar, Ghusuri, and Jadavpur.

At Dasnagar (Figure 3b) and Ghusuri (Figure 3c), peak T/B ratios ($>$ 90th percentile, representing T/B > 3.0–5.0) align along westerly and north-westerly wind sectors. These directions coincide with industrial surface coating and solvent extraction plants, demonstrating that industrial solvent evaporation plumes are transported from west to east across the river. Conversely, at Jadavpur (Figure 3d), T/B ratio peaks remain localized, confirming the dominance of combustion sources.

3.5.3 Photochemical and Particulate CPF Vectors

Figures 4–6 illustrate CPF vectors for secondary photochemical regime indicators (O_3/NO_x, $\sum$BTEX/NO_x) and fine particulate ratios ($PM_{2.5}/PM_{10}$).

Photochemical O_3/NO_x ratios (Figure 4) peak during periods of south-westerly marine airflow in pre-monsoon months and during midday hours under high solar insolation. High fine particulate ratios ($PM_{2.5}/PM_{10} > 0.65$–0.75, Figure 6) align with north-northeasterly continental airflow, confirming the advection of secondary fine aerosol plumes down the Gangetic corridor during winter.



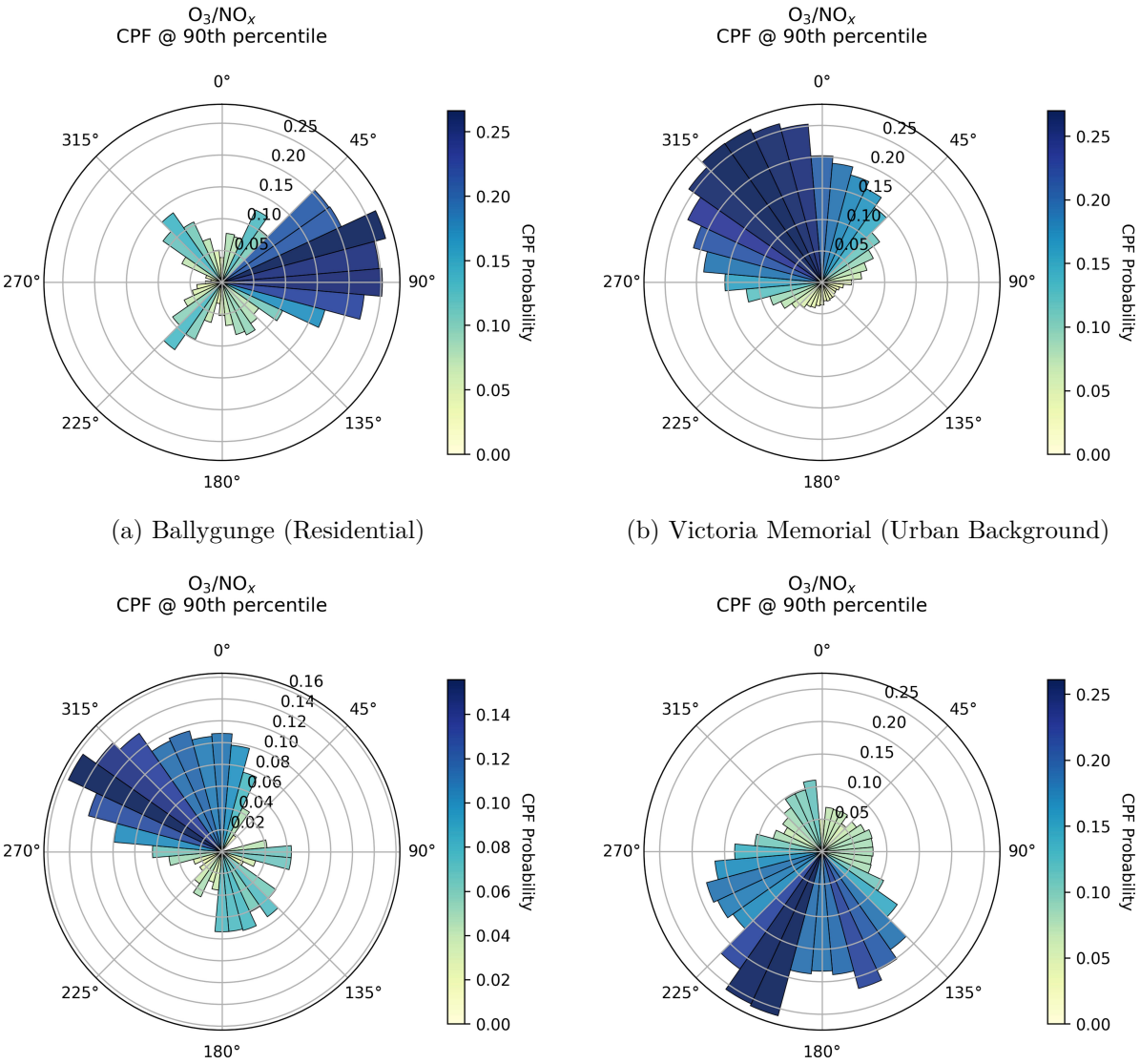
(a) Ballygunge (Residential Corridor)

(b) Dasnagar (Heavy Industrial Foundry)

(c) Ghusuri (Heavy Industrial Solvent Plumes)

(d) Jadavpur (Vehicular Combustion Corridor)

Fig. 3 Conditional Probability Function (CPF) polar plots for Toluene-to-Benzene (T/B) diagnostic emission ratios across contrasting land-use environments



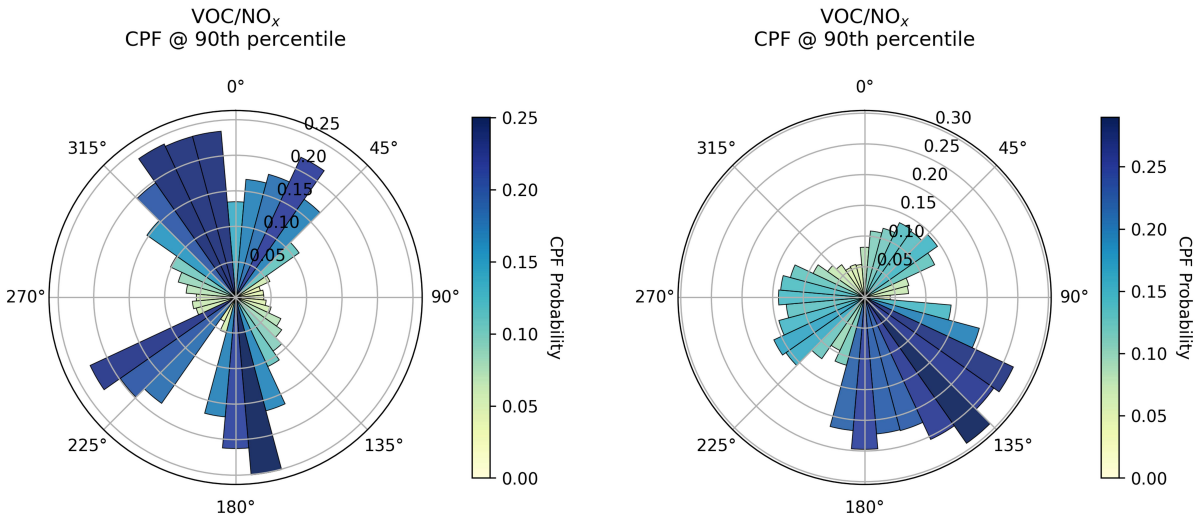
(a) Ballygunge (Residential)

(b) Victoria Memorial (Urban Background)

(c) Dasnagar (Heavy Industrial)

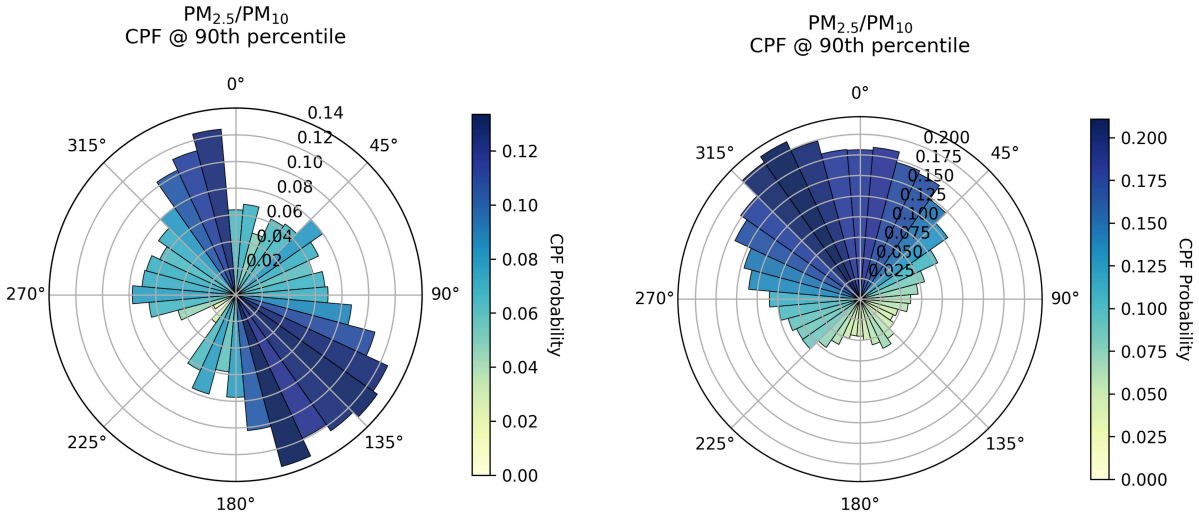
(d) Ghusuri (Heavy Industrial)

Fig. 4 Conditional Probability Function (CPF) polar plots for O_3/NO_x photochemical ratios across representative monitoring stations in Kolkata and Howrah



(a) Ballygunge (Residential) (b) Dasnagar (Heavy Industrial)

Fig. 5 Conditional Probability Function (CPF) polar plots for $\sum$BTEX/NO_x chemical regime indicators at contrasting residential and industrial microclimates



(a) Ballygunge (Residential) (b) Victoria Memorial (Urban Background)

Fig. 6 Conditional Probability Function (CPF) polar plots for fine-to-coarse particulate ratios ($PM_{2.5}/PM_{10}$) identifying stagnant northerly winter transport

3.6 Inhalation Carcinogenic Risk Assessment and Regulatory Compliance

As reported in Tables 2 and 3, ambient benzene concentrations generate substantial chronic inhalation health risks across all 13 monitoring stations:

1. Peak Hotspot Risks: In 2024, Jadavpur recorded the highest benzene concentration ($18.07\,\mu$g m^{-3}), yielding an Incremental Lifetime Cancer Risk of 108.43×10^{-6} (1.08×10^{-4}) under the primary WHO Inhalation Unit Risk model ($\mathrm{ILCR_{WHO}}$) and 90.35×10^{-6} under the USEPA IRIS midpoint estimate ($\mathrm{ILCR_{IRIS}}$), exceeding the 1×10^{-4} threshold for intolerable public health risk. In 2025, Jadavpur risks remained elevated at 87.65×10^{-6} (WHO) and 73.05×10^{-6} (IRIS).

2. Network-Wide De Minimis Exceedance: Universal exceedance of the 1×10^{-6} negligible screening threshold occurred across 100% of monitoring stations in both years. Even at the cleanest background locations (Victoria Memorial 2025: $1.70\,\mu$g m^{-3}; Fort William 2024: $2.24\,\mu$g m^{-3}), lifetime cancer risks reached 10.17×10^{-6} and 13.45×10^{-6} (WHO), respectively.

3. CPCB Statutory NAAQS Exceedances: In 2024, under the statutory 75% quarterly completeness rule, four full-year stations exceeded India's annual benchmark of $5.0\,\mu$g m^{-3}: Jadavpur ($18.07\,\mu$g m^{-3}, +261%), Ballygunge ($6.33\,\mu$g m^{-3}, +27%), Belur Math ($5.33\,\mu$g m^{-3}, +7%), and Padmapukur ($5.11\,\mu$g m^{-3}, +2%). In addition, two partial-year operational records also recorded average concentrations above $5.0\,\mu$g m^{-3} during their monitored windows: Botanical Garden ($9.63\,\mu$g m^{-3}, 39.12% capture) and Dasnagar ($7.44\,\mu$g m^{-3}, 19.48% capture). In 2025, among the 11 stations satisfying the $\geq 75\%$ quarterly completeness requirement (with 10 stations exceeding 85% capture), Jadavpur ($14.61\,\mu$g m^{-3}, +192%) and Botanical Garden ($8.29\,\mu$g m^{-3}, +66%) remained in persistent non-compliance. Two stations—Fort William (56.84% capture) and Padmapukur (74.42% capture)—experienced extended monitoring gaps exceeding 50 days during the summer and monsoon periods and are designated as not assessable for formal statutory annual compliance under the stated completeness rule.

4. Non-Carcinogenic Hazard: Chronic Hazard Quotients (HQ) remained below unity across all stations ($\mathrm{HQ} = 0.05$–0.60 in 2024; 0.06–0.49 in 2025), indicating that non-carcinogenic hematological toxicity thresholds ($\mathrm{RfC} = 30\,\mu$g m^{-3}) were not breached on an annual mean basis.

4 Discussion

4.1 Atmospheric Dynamics and Trans-Riverine Transport Corridors

The integration of 13 continuous chromatography monitoring stations provides empirical evidence of atmospheric transport across the Hooghly River. During winter, synoptic north-westerly and westerly winds transport industrial foundry plumes, metal casting emissions, and solvent evaporation from Howrah (Dasnagar, Ghusuri) across the river into downwind receptor zones in Kolkata (Figure 2). When air parcels cross the Hooghly River, thermal differentials between the warmer river surface and cooler land surfaces can induce localized river-breeze circulations that modulate plume impaction along the riverbanks (e.g., Belur Math, Botanical Garden) (Kar et al., 2020).

The high benzene loading observed at Botanical Garden ($9.63\,\mu$g m^{-3} in 2024; $8.29\,\mu$g m^{-3} in 2025) demonstrates this phenomenon. Although Botanical Garden is a designated green sanctuary, it is positioned directly downwind of the Howrah industrial casting zone under dominant westerly wind corridors. Elevated T/B ratios (1.65 in 2024) and high ethylbenzene concentrations ($7.42\,\mu$g m^{-3}) at Botanical Garden confirm the advection of industrial solvent plumes across the river corridor rather than localized emissions within the parkland.

4.2 The Photochemical Paradox: Decoupling Ozone Reactivity from Toxicological Hazard

A central finding of this study is the marked divergence between photochemical ozone reactivity and inhalation carcinogenic risk. Air quality governance strategies frequently treat total VOCs as a monolithic pollutant class. However, our findings demonstrate that:

1. Benzene accounts for 100% of the quantified unit-risk carcinogenic inhalation burden across all demographic groups, yet contributes on average only 6.2% of network BTEX-derived Ozone Formation Potential ($\mathrm{OFP}_{\mathrm{Total}}$).

2. Toluene and Xylenes collectively drive $> 85\%$ of total Ozone Formation Potential, yet possess orders of magnitude lower chronic inhalation toxicity indices.

This divergence carries significant implications for urban environmental policy:

- A regulatory strategy aimed solely at tropospheric ozone abatement will achieve maximum returns by curtailing reactive alkylbenzene emissions—namely, *m*, *p*-xylene, *o*-xylene, and toluene—through solvent recovery units in industrial painting, metal fabrication, and printing facilities.

- Conversely, such an ozone-focused strategy would yield negligible reductions in population leukemia risk unless benzene emissions are specifically targeted. Mitigating

benzene requires dedicated interventions: Stage I and Stage II Vapor Recovery Systems (VRS) at retail petrol dispensing stations, strict anti-adulteration fuel testing, anti-idling restrictions in street canyons, and targeted vehicular emission control.

4.3 Regional and Global Comparisons

Table 5 compares ambient BTEX concentrations and diagnostic T/B ratios observed in Kolkata–Howrah with published values from major South Asian, East Asian, and global metropolitan centers.

Table 5. Comparison of Ambient BTEX Concentrations (μg m^{-3}) and T/B Diagnostic Ratios across Global and Indian Megacities.

City / Region	Study Period / Typology	Benzene	Toluene	T/B	Reference
Kolkata (Jadavpur)	2024 Continuous Urban Traffic	18.07	8.53	0.47	This Study
Howrah (Dasnagar)	2024 Winter Heavy Industrial	7.44	14.41	1.94	This Study
Kolkata (Network)	2024–2025 Conurbation Mean	5.17	6.84	1.32	This Study
Delhi, India	Urban Mixed Corridor	14.20	23.50	1.65	Tiwari et al. (2010)
Mumbai, India	Industrial / Traffic Mixed	8.60	19.40	2.26	Srivastava et al. (2005)
Kolkata, India	Kerbside Passive Monitoring	22.30	14.70	0.66	Majumdar et al. (2011)
Beijing, China	Urban Traffic Corridor	4.10	8.30	2.02	Barletta et al. (2005)
Pearl River Delta, China	Regional Ambient Network	3.80	11.20	2.95	Ho et al. (2004)
Paris, France	Urban Background	0.80	2.10	2.62	Deguen and Zmirou-Navier (2010)
Los Angeles, USA	Urban Airshed Network	0.90	3.40	3.78	Batterman et al. (2020)

Kolkata's peak benzene loadings (14.61–18.07 μg m^{-3} at Jadavpur) remain among the highest reported in global megacity literature, exceeding levels observed in North American and European cities by more than an order of magnitude. Ambient concentrations align with historical values reported by Majumdar et al. (2011) and Chattopadhyay et al. (2010), indicating that despite progressive fuel improvements (such as the introduction of BS-VI fuel standards in India in 2020), localized street canyon trapping and evaporative losses maintain high benzene loadings at traffic junctions.

4.4 Exposure Assessment Realism and Screening Risk Interpretation

The inhalation cancer risk estimates reported herein (ILCR $= 8.94 \times 10^{-6}$ to 108.43×10^{-6} under the WHO unit risk benchmark; 7.45×10^{-6} to 90.35×10^{-6} under the USEPA IRIS midpoint estimate) must be interpreted as upper-bound screening-level regulatory benchmarks rather than deterministic clinical cancer diagnoses in the living population (USEPA, 2009; WHO, 2000, 2010). Standard continuous unit risk models evaluate outdoor concentration assuming continuous lifetime ambient exposure. Several physical factors modulate real-world human exposure:

1. Indoor Attenuation: Urban residents spend approximately 80%–90% of their daily lifetime indoors. Residential building envelopes attenuate outdoor-derived VOCs; indoor-to-outdoor (I/O) benzene concentration ratios typically range between 0.55

and 0.80 in non-smoking households without indoor solvent sources (WHO, 2010; Deguen and Zmirou-Navier, 2010). This attenuation reduces cumulative lifetime intake by 20%–40% relative to outdoor station measurements.

2. Human Spatial Mobility: Commuting patterns and daily mobility disperse personal exposure across multiple microclimates, preventing continuous lifetime residence at roadside peak concentrations.

3. Occupational Vulnerability: While general population risks are modulated by indoor buffering, occupational cohorts—such as traffic police officers, auto-rickshaw and taxi drivers, street vendors, and roadside retail workers—experience unattenuated breathing-zone concentrations for 8 to 14 hours daily, representing a high-risk group that warrants targeted medical surveillance (Chattopadhyay et al., 2010; Batterman et al., 2020).

4.5 Study Strengths and Limitations

This study provides the first continuous, multi-station, multi-year chromatographic assessment of speciated BTEX dynamics across 13 diverse microclimates in eastern India. Key strengths include verified machine-precision stoichiometric closure across 721,193 telemetry records, objective deconstruction of seasonal sampling bias at Dasnagar, contemporary concentration-based Inhalation Unit Risk modeling (WHO and USEPA RAGS Part F), and integration of Carter MIR reactivity modeling.

Several scientific limitations must be acknowledged:

1. VOC speciation was restricted to five monoaromatic hydrocarbons (BTEX) quantified by the online GC-PID systems. Highly reactive aliphatic alkenes (such as 1,3-butadiene, isoprene) and oxygenated VOCs (formaldehyde, acetaldehyde) were not monitored, meaning that total photochemical reactivity represents a conservative lower bound.

2. Fixed surface monitoring stations (3.5–10 m) do not capture vertical boundary-layer concentration gradients. Co-located vertical profiling via Differential Optical Absorption Spectroscopy (DOAS) or tethered balloon sondes would strengthen the physical understanding of nocturnal inversion decoupling.

3. Three stations in 2024 and two stations in 2025 had incomplete annual data capture, requiring seasonal qualification of annual metrics.

5 Conclusions and Environmental Policy Implications

This study delivers an evidence-based assessment of monoaromatic hydrocarbon speciation, photochemical reactivity, directional dispersion corridors, and chronic inhalation health risks across 13 urban microclimates in the Kolkata–Howrah megacity airshed. Ambient benzene concentrations exceeded India's statutory benchmark ($5.0\,\mu$g m^{-3}) at four full-year stations and two partial-year seasonal records in 2024, with Jadavpur ($18.07\,\mu$g m^{-3}) and Botanical Garden ($9.63\,\mu$g m^{-3}) exhibiting substantial non-compliance that persisted through 2025. Incremental Lifetime Cancer Risk (ILCR) evaluated under the contemporary concentration-based Inhalation Unit Risk framework exceeded the regulatory de minimis benchmark of 1×10^{-6} across 100% of monitoring stations, reaching screening levels above 1×10^{-4} (108.4×10^{-6} under WHO IUR) at congested vehicular intersections.

Photochemical reactivity analysis demonstrated a marked policy divergence: while Benzene drives 100% of the quantified unit-risk carcinogenic burden, Toluene and Xylenes dominate BTEX-based Ozone Formation Potential ($> 85\%$ OFP). Directional CPF polar vectors indicated that westerly transport corridors channel industrial solvent and foundry emissions across the Hooghly River, while north-northeasterly flows transport regional continental drainage during winter inversions. It should be emphasized that CPF is an empirical receptor-oriented screening diagnostic based on conditional probabilities rather than a definitive source-apportionment mass-balance model.

Based on these findings, we recommend the following policy interventions for air quality authorities under India's National Clean Air Programme (NCAP):

1. Mandatory Vapor Recovery Systems (VRS): Rigorous enforcement and verification of Stage I and Stage II VRS installation across all retail fuel dispensing stations in the metropolitan area, coupled with fuel anti-adulteration inspections.

2. Industrial Solvent Capture and Recovery: Regulatory mandates requiring enclosed spray-painting booths, solvent vapor recovery units, and thermal oxidizers across Howrah foundry, casting, and coating enterprises.

3. Traffic Channelization and Anti-Idling: Traffic engineering interventions at high-density commercial intersections (Jadavpur, Ballygunge, RBU) to reduce stop-and-go congestion and eliminate prolonged vehicle idling.

References

Ashbaugh LL, Malm WC, Sadeh WZ (1985) A methodology for establishing the relationship between air quality and meteorological variables. Atmospheric Environment 19(1):129–135, https://doi.org/10.1016/0004-6981(85)90145-3

Atkinson R, Arey J (2003) Atmospheric degradation of volatile organic compounds. Chemical Reviews 103(12):4605–4638, https://doi.org/10.1021/cr0206420

Balakrishnan K, et al. (2019) The impact of air pollution on deaths, disease burden, and life expectancy across the states of india. The Lancet Planetary Health 3(1):e26–e39

Barletta B, Meinardi S, Rowland FS, Chan CY, Wang X, Zou S, Chan LY, Blake DR (2005) Volatile organic compounds in 43 Chinese cities. Atmospheric Environment 39(32):5979–5990, https://doi.org/10.1016/j.atmosenv.2005.06.029

Batterman S, Berrocal VJ, Milando C, Gilani O, Arunachalam S, Zhang K (2020) Enhancing models and measurements of traffic-related air pollutants for health studies using dispersion modeling and bayesian data fusion. Bucknell Digital Commons (Bucknell University) (202):1–63

Calvert JG, Atkinson R, Becker KH, Kamens RM, Seinfeld JH, Wallington TJ, Yarwood G (2002) The Mechanisms of Atmospheric Oxidation of Aromatic Hydrocarbons. Oxford University Press, New York

Camredon M, Aumont B, Lee-Taylor J, Madronich S (2007) The SOA/VOC/NO_x system: an explicit model of secondary organic aerosol formation. Atmospheric chemistry and physics 7(21):5599–5610, https://doi.org/10.5194/acp-7-5599-2007

Carter WPL (1994) Development of ozone reactivity scales for volatile organic compounds. Journal of the Air & Waste Management Association 44(7):881–899, https://doi.org/10.1080/1073161X.1994.10467290

Carter WPL (2010) Development of the SAPRC-07 chemical mechanism and updated ozone reactivity scales. Atmospheric Environment 44(40):5324–5335, https://doi.org/10.1016/j.atmosenv.2010.09.009

Chameides WL, Fehsenfeld F, Rodgers MO, Cardelino C, Martinez J, Parrish D, Lonneman W, Lawson TR, Rasmussen RA, Zimmerman P, Greenberg J, Middleton P, Wang T (1992) Ozone precursor relationships in the ambient atmosphere. Journal of Geophysical Research: Atmospheres 97(D5):6037–6055, https://doi.org/10.1029/91JD03014

Chattopadhyay G, Samanta G, Roy S (2010) Determination of benzene, toluene and xylene in ambient air of Kolkata for assessing toxic human exposure. Environmental Monitoring and Assessment 166(1):475–487, https://doi.org/10.1007/s10661-009-1016-1

Das M, et al. (2020) Assessing the immediate impact of covid-19 lockdown on the air quality of kolkata and howrah, west bengal, india. Environment, Development and Sustainability 23(7):10115–10134, https://doi.org/10.1007/s10668-020-00985-7

Deguen S, Zmirou-Navier D (2010) Social inequalities resulting from health risks related to ambient air quality–a european review. European Journal of Public Health 20(1):27–35, https://doi.org/10.1093/eurpub/ckp220

Dutta D, Pal SK (2022) Prediction and assessment of the impact of covid-19 lockdown on air quality over kolkata: a deep transfer learning approach. Environmental Monitoring and Assessment 195(1):223–223, https://doi.org/10.1007/s10661-022-10761-x

Ghosh B, Barman HC, Padhy PK (2023) Analysis of spatiotemporal distribution of air quality index (aqi) in the state of west bengal, india from 2016 to 2021. Discover Atmosphere 1(1), https://doi.org/10.1007/s44292-023-00001-3

Ho KF, Lee SC, Guo H, Tsai WY (2004) Seasonal and diurnal variations of volatile organic compounds (VOCs) in the Pearl River Delta Region, China. Atmospheric Environment 38(33):5635–5646, https://doi.org/10.1016/j.atmosenv.2004.06.027

IARC (2018) Benzene, IARC Monographs on the Evaluation of Carcinogenic Risks to Humans, vol 120. International Agency for Research on Cancer, Lyon, France

Kar S, Dey S, et al. (2020) Significant impacts of covid-19 lockdown on urban air pollution in kolkata (india) and amelioration of environmental health. Environment, Development and Sustainability 23(6):8790–8806, https://doi.org/10.1007/s10668-020-00898-5

Karmakar J (2020) Air pollution in kolkata: Emerging challenges and dynamics. Journal of Atmospheric Science Research 3(4):1–9, https://doi.org/10.30564/jasr.v3i4.2231

Kumar A, et al. (2018) Assessment of air quality status and its health risk estimation in kolkata during winter smog events. Environmental Science and Pollution Research 25(10):9474–9488

Lan Q, Zhang L, Li GL, Vermeulen R, Waidyanatha S, Johnson AE, Rothman N, Smith MT, Rappaport SM, Shen M, et al. (2004) Hematotoxicity in workers exposed to low levels of benzene. Science 306(5702):1774–1776, https://doi.org/10.1126/science.1102443

Majumdar D, Mukhopadhyay K, Mukherjee AK, Sen S (2011) Assessment of volatile organic compounds (VOCs) in ambient air of Kolkata for estimating health risks. Environmental Science and Pollution Research 18(4):572–580, https://doi.org/10.1007/s11356-010-0399-2

Mondal S, Chatterjee S, Maity R, Gain D, Mazumdar D (2023) Imprints of vehicular pollution in roadside dust from kolkata, india: insights from magnetic susceptibility,

geo-statistical and sem studies. Current Science 124(1):56–56, https://doi.org/10.18520/cs/v124/i1/56-62

Monks PS, Archibald AT, Colette A, Cooper OR, Coyle M, Derwent RG, Fowler D, Granier C, Law KS, Mills G, Stevenson DS, Tarasova O, Thouret V, von Schneidemesser E, Sommariva R, Wild O, Williams ML (2015) Tropospheric ozone and its precursors from the urban to the global scale from air quality to short-lived climate forcer. Atmospheric chemistry and physics 15(15):8889–8973, https://doi.org/10.5194/acp-15-8889-2015

Pekey H, Yilmaz K (2011) The use of source apportionment to assess the contribution of VOCs to ambient levels in an industrialised area. Chemosphere 84(1):160–170, https://doi.org/10.1016/j.chemosphere.2011.02.044

Rai P, Furger M, Haddad IE, Kumar V, Wang L, Singh A, Dixit K, Bhattu D, Petit J, Ganguly D, Rastogi N, Baltensperger U, Tripathi SN, Slowik JG, Prévôt ASH (2020) Real-time measurement and source apportionment of elements in delhi's atmosphere. The Science of The Total Environment 742:140332–140332, https://doi.org/10.1016/j.scitotenv.2020.140332

Rinsky RA, Smith AB, Hornung R, Filloon TG, Young RJ, Okun AH, Landrigan PJ (1987) Benzene and leukemia: an epidemiologic risk assessment. New England Journal of Medicine 316(17):1044–1050, https://doi.org/10.1056/NEJM198704233161702

Roy R, et al. (2024) Ozone trends and their sensitivity in global megacities under the warming climate. Nature Communications 15(1):1–12, https://doi.org/10.1038/s41467-024-54490-w

Sarkar M, Das A, Mukhopadhyay S (2020) Assessing the immediate impact of covid-19 lockdown on the air quality of kolkata and howrah, west bengal, india. Environment Development and Sustainability 23(6):8613–8642, https://doi.org/10.1007/s10668-020-00985-7

Sillman S, He D (2002) Some theoretical results concerning O_3–NO_x–VOC chemistry and NO_x–VOC indicators. Journal of Geophysical Research Atmospheres 107(D22), https://doi.org/10.1029/2001jd001123

Smith MT (2010) Advances in understanding benzene leukemogenicity and genotoxicity. Annual Review of Public Health 31:133–148, https://doi.org/10.1146/annurev.publhealth.012809.103646

Srivastava A, Sengupta B, Dutta SA (2005) Source apportionment of volatile organic compounds in Mumbai, India. Atmospheric Environment 39(37):6839–6847, https://doi.org/10.1016/j.atmosenv.2005.07.025

Tan Z, Lu K, Jiang M, Su R, Wang H, Lou S, Fu Q, Zhai C, Tan Q, Yue D, Chen D, Wang Z, Xie S, Zeng L, Zhang Y (2019) Daytime atmospheric oxidation capacity in four chinese megacities during the photochemically polluted season: a case study based on box model simulation. Atmospheric chemistry and physics 19(6):3493–3513, https://doi.org/10.5194/acp-19-3493-2019

Tiwari V, Hanai Y, Masunaga S (2010) Ambient levels of volatile organic compounds in the urban atmosphere of Delhi, India. Atmospheric Research 95(2-3):258–267, https://doi.org/10.1016/j.atmosres.2009.10.007

USEPA (1989) Risk assessment guidance for superfund (rags), volume i: Human health evaluation manual (part a). Tech. Rep. EPA/540/1-89/002, Office of Emergency and Remedial Response, U.S. Environmental Protection Agency, Washington, DC

USEPA (1997) Health effects assessment summary tables (heast): Fy 1997 update. Tech. Rep. EPA-540-R-97-036, Office of Solid Waste and Emergency Response, U.S. Environmental Protection Agency, Washington, DC

USEPA (2000) Toxicological review of benzene (casrn 71-43-2) in support of summary information on the integrated risk information system (iris). National Center for Environmental Assessment, Office of Research and Development, U.S. Environmental Protection Agency, Washington, DC, URL https://iris.epa.gov/ChemicalLanding/&substance_nmbr=276

USEPA (2009) Risk assessment guidance for superfund (rags), volume i: Human health evaluation manual (part f, supplemental guidance for inhalation risk assessment). Tech. Rep. EPA-540-R-070-002, Office of Superfund Remediation and Technology Innovation, U.S. Environmental Protection Agency, Washington, DC

Venkataraman C, Bräuer M, Tibrewal K, Sadavarte P, Ma Q, Cohen A, Chaliyakunnel S, Frostad J, Klimont Z, Martin RV, Millet DB, Philip S, Walker K, Wang S (2018) Source influence on emission pathways and ambient $PM_{2.5}$ pollution over India (2015–2050). Atmospheric chemistry and physics 18(11):8017–8039, https://doi.org/10.5194/acp-18-8017-2018

Volkamer R, Sheehy PM, Molina LT, Molina MJ (2010) Oxidative capacity of the mexico city atmosphere – part 1: A radical source perspective. Atmospheric chemistry and physics 10(14):6969–6991, https://doi.org/10.5194/acp-10-6969-2010

WHO (2000) Air Quality Guidelines for Europe, 2nd edn. WHO Regional Publications, European Series, No. 91, World Health Organization, Regional Office for Europe, Copenhagen

WHO (2010) WHO Guidelines for Indoor Air Quality: Selected Pollutants. World Health Organization, Regional Office for Europe, Copenhagen

Xue L, Wang T, Gao J, Ding A, Zhou X, Blake DR, Wang X, Saunders SM, Fan S, Zuo H, Zhang QZ, Wang WX (2014) Ground-level ozone in four chinese cities: precursors, regional transport and heterogeneous processes. Atmospheric chemistry and physics 14(23):13175–13188, https://doi.org/10.5194/acp-14-13175-2014

Zhang Q, Yuan B, Shao M, Wang X, Lü S, Lu K, Wang M, Chen L, Chang CK, Liu SC (2014) Variations of ground-level O_3 and its precursors in Beijing in summertime between 2005 and 2011. Atmospheric chemistry and physics 14(12):6089–6101, https://doi.org/10.5194/acp-14-6089-2014

Statements and Declarations

Funding: The author declares that no funds, grants, or other support were received during the preparation of this manuscript.

Competing Interests: The author has no relevant financial or non-financial interests to disclose.

Author Contributions: S.S. conceived the study, curated the continuous GC-PID chromatography and meteorological telemetry datasets, developed the photochemical reactivity, CPF directional vector, and inhalation risk modeling pipelines, performed the statistical validations, and wrote the manuscript.

Data Availability: Continuous ambient air quality telemetry is publicly accessible through the Central Pollution Control Board (CPCB) portal (https://app.cpcbccr.com/ccr/). All reproducible Python analysis scripts, statistical validation pipelines, and processed matrices are available from the corresponding author upon request.

Code Availability: Standalone Python analysis, CPF plotting, and risk assessment scripts are archived in the reproducibility package and are available from the corresponding author upon request.

Ethics Approval: Not applicable. This study utilizes non-human ambient atmospheric telemetry and does not involve human participants or animal subjects.

Consent to Participate: Not applicable.

Consent to Publish: Not applicable. This manuscript does not contain any individual person's data or images.

Computational Framework and AI Disclosure: All data processing, statistical modeling, and validation pipelines were implemented in Python 3.13. Generative AI tools (Anthropic Claude and Google Gemini) assisted substantially in computational script development, mathematical formalization, structuration of theoretical linkages, and manuscript drafting and language editing. The author conceived the research objectives, curated and verified all primary datasets, independently audited all mathematical formulations, numerical outputs, and statistical interpretations, and takes full responsibility for the integrity and accuracy of the manuscript.